Interpretable Intrinsic Cues for Efficient Reinforcement Learning with Large Language Models

Anonymous ACL submission

Abstract

Reinforcement learning with verifiable rewards (RLVR) has improved the reasoning ability of large language models, yet training remains costly because many rollouts contribute little to optimization relative to their heavy computational demands. This study investigates how simply leveraging interpretable and intrinsic data properties, which come at almost no additional computational cost during training, can markedly improve data efficiency for RLVR. We propose PREPO[1], an RLVR model with two complementary components. First, we use prompt perplexity as a proxy for model adaptability in learning, and adopt a schedule to guide the model from well-understood prompts to progressively challenging ones. Second, we amplify the diversity among rollouts by differentiating their relative entropy and prioritizing sequences with greater exploratory behavior. Together, these mechanisms reduce rollout demand while preserving competitive performance. On Qwen and Llama models, PREPO achieves effective results on mathematical reasoning benchmarks with up to 3× fewer rollouts than baselines. Beyond empirical gains, we provide theoretical and in-depth analyses that explain how our method improves the data efficiency of RLVR.

1 Introduction

Reinforcement learning (RL) has become central in improving the reasoning capabilities of large language models (LLMs) by optimizing self-generated rollouts [Guo et al., 2025, Team et al., 2025, Chen et al., 2025a]. Recent advances in reinforcement learning with verifiable reward (RLVR) demonstrate that it is a simple yet effective method for scaling reasoning performance [Shao et al., 2024, Yu et al., 2025]. However, applying RLVR to models that generate long reasoning traces will incur substantial computational overhead in the rollout stage, significantly hampering RL training efficiency and becoming the primary training bottleneck [Zhong et al., 2024].

The exploration of effective strategies for leveraging data in RL training remains relatively underdeveloped. Prior studies [Zhang et al., 2025, Albalak et al., 2025] have suggested using pass rate as an indicator of data difficulty to strengthen the training signal. Nonetheless, this approach often requires multiple rounds of sampling to attain a sufficiently stable measurement. In fact, it converts online rollouts into an offline context, which ultimately does not reduce the overall computational burden. Other metrics, such as human-defined criteria [Chen et al., 2025b, Parashar et al., 2025], *e.g.*, specific domains or topics, have the disadvantage of being influenced by the tagging process and by biases in human perceptions and experiences. In addition, alternative approaches often depend on auxiliary trained models or embedding techniques to reflect data semantics. We assert that these techniques not only impose significant computational and memory costs but also introduce mismatches and limited applicability across diverse policy models and training paradigms. Furthermore, they overlook the inherent dynamism of the RL training process, lagging far behind the pace of training updates. As a remedy, other methods incorporate historical information from training to reflect the dynamic nature of data. Nevertheless, it increases memory requirements for the RL framework and introduces extraneous noise during training.

A natural way to improve training efficiency is to select data, i.e., prune uninformative prompts or rollouts while preserving those that drive learning. There are emerging approaches based on parameterized modeling [Qu et al., 2025], replay buffers [Liu et al., 2025], or selective rollout execution [Zheng et al., 2025]. Instead of being aided by inductive biases from both humans and external models, we address this long-standing research question from

[1]We will release data and codes soon upon acceptance.

a new perspective:

Can the intrinsic data properties deriving from the training process improve the efficiency of RLVR?

In this study, we propose a simple method with almost negligible computation cost, Perplexity-schedule with Relative-Entropy Policy Optimization (PREPO), a method that combines a perplexity-based schedule with sequence-level entropy weighting to realize *intrinsic exploration*. Specifically, PREPO traces perplexity *before* rollout generation to prune the prompts, and applies entropy weighting *after* rollout generation to emphasize uncertain responses. It is worth noting that metrics collected during standard RL training can be reused to compute both components, thereby ensuring computational efficiency of our method. Moreover, our method is coherently integrated with the policy model and training process, offering a favorable trade-off between suitability and flexibility. Beyond that, our approach uncovers the intrinsic nature of data during RL training, providing fine-grained interpretability of training dynamics. Across Qwen and Llama models, PREPO surpasses existing data-pruning baselines and remains competitive with the baseline, while reducing rollout usage by more than 40% (see Fig. 1 for Qwen2.5-Math-7B). These results show that RLVR can be made substantially more efficient by leveraging the intrinsic properties of prompt and rollout data.

2 Related Work

Data efficiency in RLVR. A growing body of work has explored data efficiency for RLVR, with particular attention to online data selection. Unlike offline methods that require pretraining or costly rollouts to estimate sample quality [Qu et al., 2025, Zhang et al., 2025, Chen et al., 2025b, Kamalloo et al., 2025], online approaches aim to reduce overhead by dynamically filtering or prioritizing samples during training. Online difficulty filtering [Bae et al., 2025] removes prompts that contribute little to reasoning improvement, while predictive prompt allocation [Qu et al., 2025] directs rollouts toward more promising inputs. Curriculum-based strategies further adapt training to the model's evolving competence [Zhang et al., 2025, Chen et al., 2025b]. Other online selection approaches prioritize samples using gradient-informed signals [Kamalloo et al., 2025, Chen et al., 2025c] or policy-advantage estimates [Wang and Guofeng, 2025]. Parallel efforts focus on reducing rollout redundancy during training. Down-sampling strategies [Li et al., 2025] and efficient replay buffer designs [Liu et al., 2025] lessen the burden of repeatedly training on uninformative samples. Collectively, these online methods emphasize the importance of allocating computational resources to samples that drive progress in reasoning, a goal that aligns with the direction of our work.

Entropy Mechanism in RLVR. Entropy has long been studied in reinforcement learning through entropy-regularized objectives that promote exploration in control settings. Recent studies extend this idea to RLVR for reasoning LLMs. Cui et al. [2025] identify rapid entropy collapse as a major failure mode and propose covariance-based updates to slow its decay. Wang et al. [2025] show that high-entropy "forking tokens," though rare, account for most reasoning gains, highlighting entropy as a token-level signal of informativeness. Cheng et al. [2025] incorporates a clipped, gradient-detached entropy term into the advantage function, encouraging more exploratory responses but introducing additional hyperparameters. Building on these insights, we propose a parameter-free approach to reinforce entropy-driven exploration in RLVR. A related line of work explores weighting in policy-gradient updates through truncated importance sampling, such as CISPO [Chen et al., 2025a]. These methods address a different dimension of RLVR optimization, and can be viewed as complementary to our focus on online data selection and entropy-based weighting.

3 Preliminary Analysis

3.1 Low-PPL Prompts Tend to Yield Higher Pass Rate

We begin by examining the relationship between prompt perplexity (PPL) and task difficulty using the DAPO-Math-17K dataset [Yu et al., 2025] (17,917 samples). For both Qwen and Llama models, Figure 2 shows a clear negative correlation between PPL and passrate@16, where passrate@16 measures the fraction of prompts solved by at least one of 16 generations. Lower-PPL prompts generally yield higher success rates. Table 1 correlation is statistically significant across models, suggesting that PPL can serve as a lightweight signal to identify more informative prompts for training.

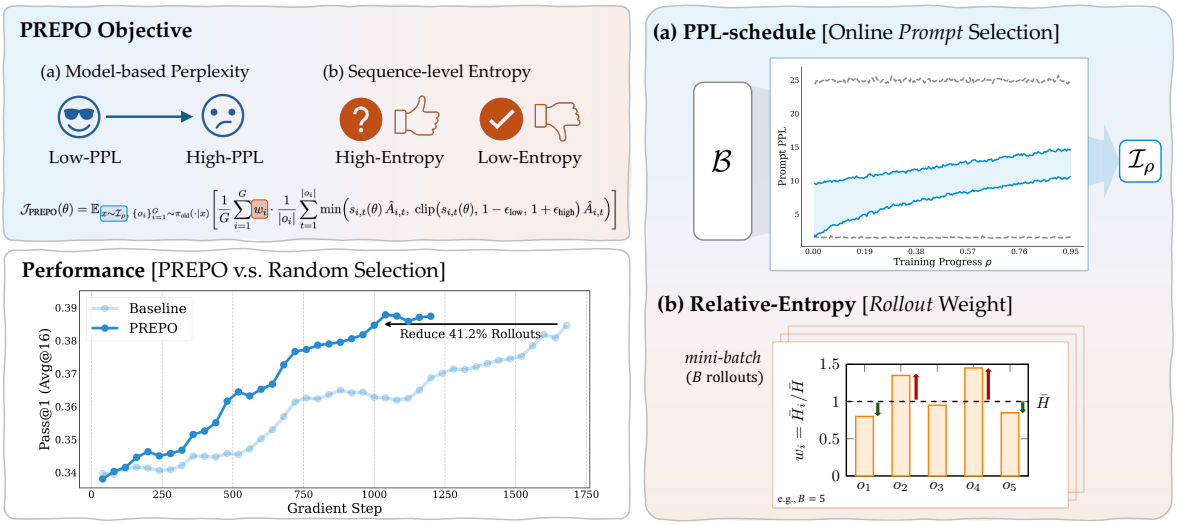

Figure 1: **Overview of PREPO.** The PREPO objective integrates perplexity-based schedule learning and sequence-level entropy weighting into a unified optimization scheme. On Qwen2.5-Math-7B, PREPO achieves higher performance while requiring only 41.2% of the rollouts used by random selection, showing improved efficiency. Specifically, PREPO has two complementary components: (a) PPL-schedule, which actively selects prompts according to model-based perplexity, starting with lower-PPL prompts *("adapted" to the model)* and progressively introducing higher-PPL ones *("obscured" to the model)* as training progresses. (b) Relative-Entropy Weighting, which adjusts rollout contributions by comparing each sequence's entropy against the batch average, amplifying the high-entropy rollouts *("novel attempts")* and downweighting the low-entropy *("regular response")*.

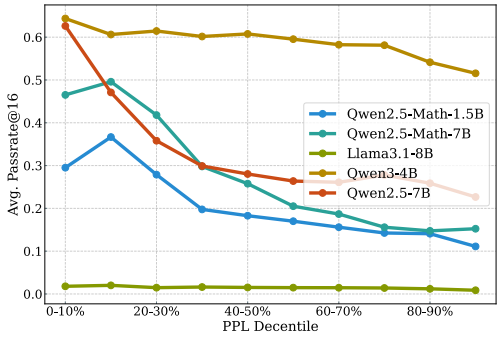

Figure 2: Prompt PPL versus average passrate@16.

Table 1: Correlation between prompt PPL and passrate@16. (*** $p < 0.001$, ** $p < 0.05$)

Qwen2.5-7B	Qwen2.5-7B	Qwen2.5-1.5B	Qwen3-4B	LLama3.1-8B
-0.233^{***}	-0.183^{**}	-0.186^{***}	-0.169^{***}	-0.199^{***}

3.2 Training Dynamics of LOW-PPL and HIGH-PPL Prompts

To better understand the role of PPL during training, we compare prompts from the lowest 20% (LOW-PPL) and highest 20% (HIGH-PPL) of the distribution (see Appendix B for examples of the two groups). Figure 3 illustrates their training dynamics on Qwen2.5-Math-7B. The two groups exhibit complementary behavior: LOW-PPL prompts drive rapid improvements in reward and validation accuracy during early training, though at the cost of faster entropy collapse, whereas HIGH-PPL prompts preserve entropy and lower zero-advantage ratio, yielding stronger performance in later stages.

These trends are consistent across other Qwen models (Appendix C). Specifically, (a) HIGH-PPL prompts are associated with higher entropy, (b) LOW-PPL prompts yield higher rewards and validation accuracy early on, and (c) HIGH-PPL prompts maintain exploration and ultimately close the performance gap. For Llama3.1-8B (Figure 10), a similar pattern appears, though overall performance remains limited as the validation dataset is too challenging for Llama models.

3.3 Comparison with Random Sampling

To test whether PPL-based grouping offers value beyond chance, we also compare with a random 20% subset. As shown in Figure 4, the random group consistently falls between the LOW-PPL and HIGH-PPL groups. This indicates that PPL is a non-trivial, policy-intrinsic signal that distinguishes easy prompts with high-pass rates from more challenging ones, providing a valuable basis for the design of online batch selection.

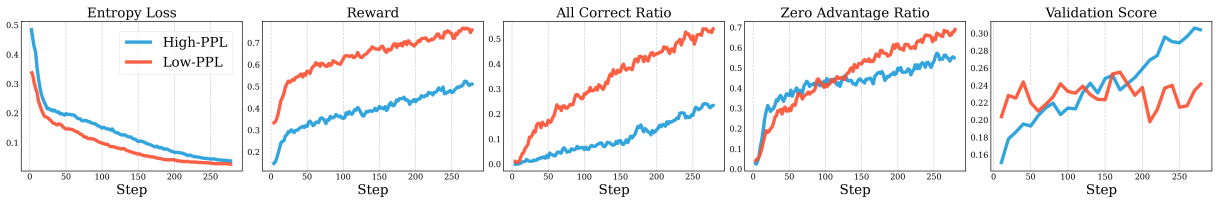

Figure 3: Training dynamics of LOW-PPL vs. HIGH-PPL prompts on Qwen2.5-Math-7B. *(a)* HIGH-PPL *prompts have higher entropy. (b)* LOW-PPL *prompts have more reward gains. (c)* LOW-PPL *prompts reach higher all-correct ratios faster. (d)* LOW-PPL *prompts show higher zero-advantage ratios in the later stage. (e)* HIGH-PPL *prompts eventually outperform* LOW-PPL *prompts.*

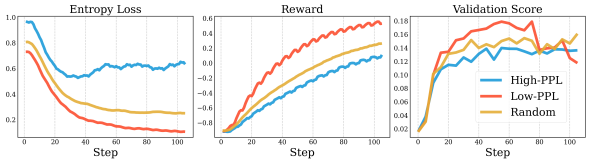

Figure 4: Comparison among LOW-PPL, HIGH-PPL, and Random Subsets. *Random lies between the two, showing that PPL-based grouping provides a meaningful pruning signal.*

4 PREPO: PPL-Schedule Relative-Entropy Policy Optimization

Building on the preliminary results, PREPO integrates a perplexity-driven schedule with entropy-based rollout weighting, forming a unified framework to improve efficiency in RLVR.

4.1 General Online Batch Selection

Let $\mathcal{B} = \{x_i\}_{i=1}^{N}$ denote the candidate batch at a training step. The goal of online batch selection is to design a mapping

$$\Phi : [0,1] \to 2^{\mathcal{B}}, \quad \rho \mapsto \mathcal{I}_\rho, \tag{1}$$

where $\rho \in [0,1]$ denotes the normalized training progress, and $\mathcal{I}_\rho \subseteq \mathcal{B}$. The mapping Φ is required to (i) explicitly depend on ρ, so that the distribution of selected samples evolves with training; (ii) the sub-batch size is fixed during training, i.e., $\forall \rho,\ |\mathcal{I}_\rho| = K$.

4.2 PPL-Schedule Online Batch Selection

For a prompt $x_i = (x_{i,1}, \dots)$, we measure its perplexity under the policy π_ρ at training progress ρ as

$$P_i(\rho) = \exp\left(-\frac{1}{|x_i|} \sum_{t=1}^{|x_i|} \log \pi_\rho(x_{i,t} \mid x_{i,<t}) \right), \tag{2}$$

where π_ρ is the model distribution at progress ρ. As π_ρ is parameterized by θ and evolves throughout training, $P_i(\rho)$ provides a model-based measure for active data selection. We then define the *PPL-schedule* sub-batch as

$$\mathcal{I}_\rho = \{\, \sigma(j) : l(\rho) \le j \le l(\rho) + K - 1 \,\}, \tag{3}$$

where σ is the permutation that sorts $\mathcal{B}$ by ascending $P_i(\rho)$. The starting index $l(\rho)$ is given by a linear schedule

$$l(\rho) = \lfloor \rho \cdot (N - K) \rfloor, \tag{4}$$

so that $\mathcal{I}_\rho$ shifts smoothly from LOW-PPL to HIGH-PPL prompts. While linear scheduling is the simplest case, a nonlinear[2] can also be used. In general, the PPL-schedule serves as an online data-selection procedure that shifts from more to less in-domain prompts as training progresses.

4.3 Relative Entropy Weighting

As shown in Section 3.2, we empirically find that training on LOW-PPL prompts accelerates reward improvement but also leads to a rapid collapse of entropy, thereby reducing exploration. To mitigate this effect during the PPL schedule, we introduce a sequence-level relative-entropy weighting scheme that adaptively emphasizes uncertain rollouts.

The token-level entropy of a rollout is defined as $H_t = -\sum_{v \in \mathcal{V}} \pi_\theta(v \mid o_{<t}, x) \log \pi_\theta(v \mid o_{<t}, x)$, where $\mathcal{V}$ is the vocabulary. For rollout i, the sequence-level entropy is the average across its tokens

$$\bar{H}_i = \bar{H}(o_i \mid x) = \frac{1}{|o_i|} \sum_{t=1}^{|o_i|} H_t. \tag{5}$$

The batch-average entropy over B rollouts is

$$\bar{H} = \frac{1}{B} \sum_{k=1}^{B} \bar{H}_k. \tag{6}$$

[2]We define a general family of nonlinear schedules as $l(\rho) = \lfloor \rho^\alpha \cdot (N - K) \rfloor$, where $\alpha \in \mathbb{R}^+$. For example, choosing $\alpha = \frac{1}{2}g$ yields a square-root schedule that transitions more quickly toward higher-PPL prompts. One (e.g., quadratic or exponential)

The relative weight assigned to rollout i is then given by

$$w_i = \frac{\bar{H}_i}{\bar{\bar{H}}}. \tag{7}$$

This formulation is scale-invariant, as a rollout's contribution depends only on its entropy relative to the batch mean. Intuitively, this design enables the model to *seek uncertainty within certainty* during the PPL schedule. While LOW-PPL prompts early in training often yield confident (low-entropy) responses, relative weighting amplifies the impact of less confident (higher-entropy) rollouts, thereby preserving exploration throughout training.

4.4 Objective Function

The PREPO objective integrates PPL-schedule filtering with relative-entropy weighting as below.

$$\mathcal{J}_{\text{PREPO}}(\theta) = \mathbb{E}_{x\sim\mathcal{I}_\rho,\ \{o_i\}_{i=1}^{G}\sim\pi_{\text{old}}(\cdot|x)} \left[\frac{1}{G}\sum_{i=1}^{G} w_i \cdot \frac{1}{|o_i|}\sum_{t=1}^{|o_i|} \min\Big(s_{i,t}(\theta)\,\hat{A}_{i,t},\ \text{clip}\big(s_{i,t}(\theta),\,1-\epsilon_{\text{low}},\,1+\epsilon_{\text{high}}\big)\,\hat{A}_{i,t} \Big) \right] \tag{8}$$

where $\mathcal{I}_\rho$ is the PPL-schedule-filtered batch of prompts at training progress ρ, w_i encodes the relative entropy of rollout i at the current micro-batch, $s_{i,t}(\theta)$ is the token-level importance ratio,$s_{i,t}(\theta) = \frac{\pi_\theta(o_{i,t}|x,o_{i,<t})}{\pi_{\text{old}}(o_{i,t}|x,o_{i,<t})}$, and $\hat{A}_{i,t}$ is the group-based advantage estimate, $\hat{A}_{i,t} = \frac{r_i - \text{mean}(\{r_j\}_{j=1}^{G})}{\text{std}(\{r_j\}_{j=1}^{G})}$.

5 Experiments

5.1 Setups

We benchmark PREPO against three baselines: Random selection, Dynamic Sampling (DS) [Yu et al., 2025], and GRESO [Zheng et al., 2025] (detailed in Appendix D). Our evaluation covers multiple models: Qwen2.5-7B [Team, 2024], Qwen2.5-Math-1.5B and Qwen2.5-Math-7B [Yang et al., 2024], Qwen3-4B (non-thinking) [Yang et al., 2025], and Llama3.1-8B [Dubey et al., 2024]. For training data, we use DAPO-Math-17K [Yu et al., 2025] and MATH500 [Lightman et al., 2023a] with a total of 18,417 training samples.

Training and Evaluation. All models are trained using the `verl` [Sheng et al., 2025], with `vLLM` [Kwon et al., 2023] employed for rollout generation to ensure efficient inference. For the Qwen models, we evaluate them on four benchmarks, including AIME25 [Art of Problem Solving, 2025] (30 samples), AIME24 [Art of Problem Solving, 2024] (30 samples), MATH500 [Lightman et al., 2023b] (500 samples), and OlympiadBench [He et al., 2024] (8,476 samples), which cover a diverse range of mathematical reasoning challenges. The Llama model is evaluated on MATH500 [Lightman et al., 2023b] and GSM8K [Cobbe et al., 2021] (1,319 samples). We evaluate all models using *pass@1 (avg16)*, i.e., the accuracy of the top-1 response averaged over 16 generations, with temperature 1. We evaluate models every 50 training steps and report the best average performance on all benchmarks.

Experiment Configuration. For the Qwen2.5-Math models, we use a maximum context length of 4096 tokens, matching their supported limit. For Qwen3-4B and Llama3.1-8B, we set the context length to 32,768 tokens. Rollouts are generated with temperature as 1 using `vLLM`, producing 8 responses per prompt. For PREPO, Random, and GRESO, we adopt an online selection ratio of $K/N = 20\%$ at each training step, where the candidate batch size (N) is 1280 and the actual batch size (K) is fixed at 256. For GRESO, we set the targeted zero-variance percentage as 50%. For DS, the candidate batch size is 384. The mini-batch size (B) is 64 for all experiments. For all experiments, we set the clipping thresholds to $\epsilon_{\text{low}} = 0.2$ by default, with a larger $\epsilon_{\text{high}} = 0.28$ as the upper bound. The actor model is optimized with AdamW using a constant learning rate of 1×10^{-6}, momentum parameters $\beta_1 = 0.9$ and $\beta_2 = 0.999$, and a weight decay of 0.01. Following Yu et al. [2025], we omit the KL-divergence regularization term. Training is applied only to the actor parameters and parallelized with Fully Sharded Data Parallel. All experiments are conducted on 32 GPUs.

5.2 Results

PREPO achieves consistent two- to three-fold rollout reduction. As shown in Table 2 below, PREPO substantially lowers rollout usage relative to all baselines while maintaining or surpassing accuracy. On Qwen2.5-7B, PREPO reduces rollouts from over 1M (DS: 1,040K; Random: 716K; GRESO: 680K) to 304K. On Qwen2.5-Math-1.5B, it cuts the budget from several million (DS: 3.6M; Random: 3.0M; GRESO: 2.5M) down to 1.1M. Similarly, PREPO reduces rollouts to 540K on

Table 2: Performance comparison (%) on Qwen models. *For each model, the top row reports the base model's performance. Best results are highlighted in bold or underlined. K = thousand, M = million.*

Method	AIME25	AIME24	MATH	Olympiad	Avg ↑	# Rollouts ↓
Qwen2.5-7B	1.25	4.17	72.26	33.09	27.69	–
+ DS	7.92	17.55	75.50	38.91	34.97	1040K
+ Random	6.98	16.41	75.70	38.47	34.39	716K
+ GRESO	9.22	10.83	76.65	42.07	34.59	680K
+ PREPO (Ours)	10.21	16.09	76.30	39.85	**35.61**	**304K**
Qwen2.5-Math-1.5B	3.54	10.21	55.76	27.41	24.23	–
+ DS	10.83	25.83	76.40	23.33	34.10	3.6M
+ Random	20.00	16.67	76.25	30.50	35.86	3.0M
+ GRESO	15.38	20.00	76.65	24.17	34.16	2.5M
+ PREPO (Ours)	20.00	16.67	76.25	32.00	**36.23**	**1.1M**
Qwen2.5-Math-7B	9.17	20.80	72.26	39.56	35.45	–
+ DS	13.33	33.33	81.35	30.17	39.55	1664K
+ Random	10.00	26.67	77.80	43.26	39.45	905K
+ GRESO	18.33	25.83	77.80	26.83	37.46	654K
+ PREPO (Ours)	12.81	26.15	77.85	41.58	**39.59**	**540K**
Qwen3-4B	30.00	53.33	94.10	52.67	57.53	–
+ DS	63.33	66.67	95.10	58.00	70.78	688K
+ Random	60.00	70.00	96.00	59.33	71.33	553K
+ GRESO	56.67	69.17	96.40	57.33	69.89	472K
+ PREPO (Ours)	66.67	80.00	96.60	60.67	**75.99**	**348K**

Qwen2.5-Math-7B (vs. 1.66M for DS, 905K for Random, 654K for GRESO) and to 348K on Qwen3-4B (vs. 688K, 553K, and 472K, respectively).

Dynamic sampling and random selection are inefficient. Although DS sometimes yields accuracy gains, it consistently demands the largest rollout budget. For instance, on Qwen2.5-Math-1.5B, DS requires 3.6M rollouts to reach an average score of 34.10, whereas PREPO attains a higher 36.23 with only 1.1M rollouts. This confirms that DS wastes computation by discarding uninformative prompts only after rollouts are generated. Random selection occasionally performs comparably to or even better than DS, yet its rollout cost remains high. On Qwen2.5-Math-7B, for example, random selection consumes 905K rollouts to achieve 39.45, while PREPO surpasses it with 39.59 using just 540K rollouts. Overall, PREPO delivers both higher accuracy and lower cost, while also producing a more diverse set of problems than online random selection (see Appendix H.6).

GRESO improves efficiency but lags behind PREPO. GRESO reduces rollout demand by prefiltering uninformative prompts, making it more efficient than DS and Random. However, its accuracy often falls short of PREPO. For instance, on Qwen3-4B, GRESO achieves 69.89 accuracy with 472K rollouts, while PREPO reaches 75.99 with only 348K rollouts. This suggests that PREPO's intrinsic exploration signals provide a more effective alternative to heuristic rollout filtering.

PREPO generalizes across model architectures. On Llama3.1-8B (see Table 3), PREPO once again achieves the strongest results, reaching an average of 36.55 with just 115K rollouts. In contrast, DS requires nearly five times as many rollouts, with substantially lower accuracy. This confirms that PREPO generalizes effectively across model families and scales, providing a consistent advantage in both performance and efficiency.

Table 3: Performance comparison (%) on Llama. *For each model, the top row reports the base model's performance. Best results are highlighted in bold or underlined. K = thousand.*

Method	GSM8K	MATH	Avg ↑	# Rollouts ↓
Llama3.1-8B	9.53	6.05	7.79	–
+ DS	39.50	17.00	28.25	553K
+ Random	46.63	14.60	30.61	266K
+ GRESO	41.77	16.80	29.29	273K
+ PREPO (Ours)	51.10	21.81	**36.55**	**115K**

PREPO could be more effective when perplexity distributions are concentrated. We found that PREPO achieves large improvement when perplexity values are relatively compact across Qwen3-4B, and LLaMA3.1-8B. As shown in Table 4, the normalized standard deviation of those models remains below one, indicating less dispersed distributions that make perplexity-based filtering more reliable. In these cases, PREPO can better exploit the PPL-schedule to reduce rollouts.

Table 4: Normalized standard deviation of prompt perplexity (std/mean) across models. *Values above one indicate more dispersed distributions.*

Qwen2.5-7B	Qwen3-4B	LLaMA3.1-8B	Qwen2.5-Math-7B	Qwen2.5-Math-1.5B
0.73	0.65	0.75	1.23	1.02

Training Dynamics of PREPO versus the Random Baseline Figures 5 and 11 (see Appendix G) present a comparison of training dynamics between PREPO and random selection. PREPO shows a higher entropy loss, indicating stronger exploratory behavior throughout training. It also sustains a higher gradient norm while avoiding instability, suggesting more active yet controlled parameter updates. In terms of learning efficiency, PREPO reduces the proportion of rollouts with zero advantage, thereby providing more informative gradients for optimization. Furthermore, the average prompt length under PREPO decreases steadily, implying an adaptive shift from longer to shorter prompts over time. A similar trend is observed in the average response length, where PREPO generates longer outputs than the baseline across most steps on average, reflecting a longer thinking behavior.

5.3 Ablation Study

In this section, we conduct the ablation analysis to isolate the contribution of each component in PREPO. In addition to the linear PPL-schedule, we evaluate four variants: (1) linear PPL-schedule, (2) random filtering with relative-entropy weighting, (3) linear PPL-schedule combined with an entropy-regularization loss, and (4) a nonlinear PPL-schedule. The nonlinear variant follows the general form $l(\rho) = \lfloor \rho^{\alpha}(N-K) \rfloor$ with $\alpha = 0.5$, which produces a schedule that shifts more quickly toward higher-PPL prompts.

As shown in Tables 5 and 6, PREPO achieves the highest average performance across all model scales. Variants that remove or modify either component show consistent performance drops, indicating that both the perplexity-based schedule and the relative-entropy weighting contribute to PREPO's effectiveness. The nonlinear schedule performs competitively but remains slightly below the linear schedule, suggesting that the linear form is already a stable and effective design choice.

Table 5: Ablation study on Llama. Performance comparison (%) between PREPO and (1) linear PPL-schedule, (2) random filtering with relative-entropy, (3) linear PPL-schedule with entropy loss, (4) non-linear PPL-schedule with relative-entropy. *Best results are highlighted in bold or underlined.*

Model	Method	GSM8K	MATH	Avg ↑
Llama3.1-8B	PREPO	<u>51.10</u>	<u>21.81</u>	**36.55**
	w/o relative entropy	46.85	18.25	32.55
	w/o PPL-schedule	34.55	16.29	25.42
	w/ entropy loss	4.45	8.30	6.33
	w/ non-linear schedule	46.85	20.56	33.71

5.4 Alternative Selection Ratio

Figure 6a and Table 8 (see Appendix G) show the effect of varying the online batch selection ratio (K/N) with N fixed for PREPO.

The 20% ratio achieves the best average performance while also requiring the fewest rollouts. A 30% ratio is competitive on some benchmarks but less efficient, while 25% does not improve overall accuracy. Smaller ratios (15%, 10%, 5%) degrade performance and consume more rollouts. Overall, 20% strikes the best balance between accuracy and efficiency, and is adopted as the default in our experiments.

5.5 Analysis of Relative-Entropy Weights

Effective Batch Sizes Relative-entropy weighting does not increase the effective batch size (i.e., $\frac{1}{B}\sum_i w_i$); it merely redistributes gradient contributions across sequences. Since the weights are normalized by $\bar{H}$, we obtain

$$\frac{1}{B}\sum_{i=1}^{B} w_i \cdot |o_i| = \frac{1}{B\bar{H}}\sum_{i=1}^{B} |o_i|\bar{H}_i = \frac{1}{B\bar{H}}\sum_{i=1}^{B}\sum_{t=1}^{|o_i|} H_{i,t} = \frac{\sum_{i=1}^{B}|o_i|}{B}. \tag{9}$$

The token-weighted average weight equals the average sequence length. If all sequences have equal length, then $\frac{1}{B}\sum_i w_i = 1$. As shown in Figure 6b, the effective batch size for PREPO on Qwen2.5-Math-1.5B stays close to B throughout training. At the early steps, LOW-PPL prompts yield low-entropy responses, so higher-entropy rollouts receive more weight, pushing the average above B. As training advances and higher-PPL

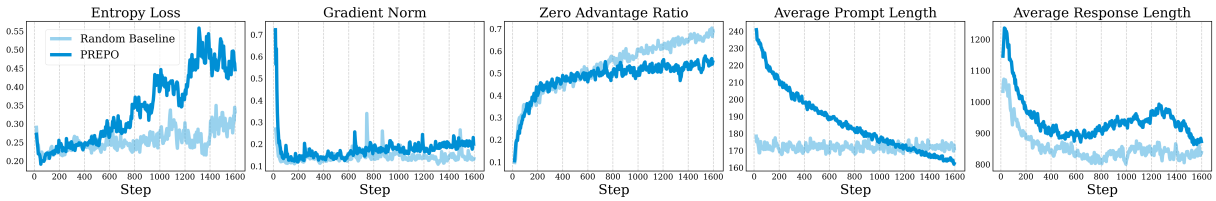

Figure 5: Full comparison between PREPO and random selection on Qwen2.5-Math-7B.

Table 6: Ablation study on Qwen. Performance comparison (%) between PREPO and (1) linear PPL-schedule, (2) random filtering with relative-entropy, (3) linear PPL-schedule with entropy loss, (4) non-linear PPL-schedule with relative-entropy. *Best results are highlighted in bold or underlined.*

Model	Method	AIME25	AIME24	MATH	Olympiad Bench	Avg ↑
Qwen2.5-Math-7B	PREPO	12.81	26.15	77.80	41.58	**39.59**
	w/o relative entropy	10.00	23.33	74.60	39.21	36.79
	w/o PPL-schedule	11.87	25.73	76.48	34.43	37.13
	w/ entropy loss	10.73	23.54	75.25	38.81	37.08
	w/ non-linear schedule	12.71	26.15	76.40	40.12	38.85
Qwen2.5-7B	PREPO	10.20	16.09	76.30	39.85	**35.61**
	w/o relative entropy	6.98	16.41	75.70	38.47	34.39
	w/o PPL-schedule	8.89	16.04	79.41	22.54	31.72
	w/ entropy loss	6.25	16.35	77.36	21.04	30.25
	w/ non-linear schedule	9.58	16.25	76.31	39.60	35.44
Qwen2.5-Math-1.5B	PREPO	20.00	16.67	76.25	32.00	**36.23**
	w/o relative entropy	10.21	15.68	72.10	30.50	32.12
	w/o PPL-schedule	11.81	13.12	70.21	30.02	31.29
	w/ entropy loss	6.46	16.56	73.77	30.99	31.95
	w/ non-linear schedule	9.15	15.83	75.85	30.26	32.77
Qwen3-4B	PREPO	66.67	80.00	96.60	60.67	**75.99**
	w/o relative entropy	64.77	72.70	90.54	59.06	71.77
	w/o PPL-schedule	64.99	77.73	95.03	57.86	73.90
	w/ entropy loss	61.10	75.17	88.39	60.54	71.28
	w/ non-linear schedule	61.45	74.47	92.37	60.67	72.24

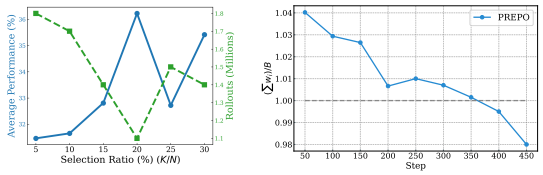

(a) Different K/N (b) Trend of effective batch size

Figure 6: More ablation studies.

prompts are used, the overall entropy rises, and normalization shifts the average slightly below B.

6 Conclusion and Future Work

This study investigated how intrinsic data properties can improve the efficiency of RLVR training. Prompt perplexity enables a natural schedule from easier to harder prompts, while sequence-level relative entropy amplifies exploratory rollouts. Integrated in PREPO, these components reduce rollout cost while maintaining or improving benchmark performance.

Beyond empirical gains, PREPO shows that RLVR can be guided by interpretable, policy-intrinsic cues rather than human heuristic or auxiliary models. This makes PREPO a practical and transparent recipe for compute-efficient RLVR, accessible even to researchers with limited resources. Future work may explore additional intrinsic signals(e.g., input token size) and combine data-driven exploration with system-level optimizations.

Appendix roadmap. Appendices B–C analyze prompt properties and training dynamics. Appendices D–F provide baseline definitions, implementation details, and evaluation procedures for reproducibility. Appendix G reports additional results, including ablations and sensitivity analyses. Appendix H discusses common concerns such as problem diversity and memorization risk.

7 Limitations

This study has several limitations that should be acknowledged. (1) response lengths were restricted to 32K tokens, leaving the applicability of PREPO to models generating substantially longer outputs an open question; and (2) the evaluation was limited to mathematical reasoning tasks, while its effectiveness in other domains remains to be explored.

References

Alon Albalak, Duy Phung, Nathan Lile, Rafael Rafailov, Kanishk Gandhi, Louis Castricato, Anikait Singh, Chase Blagden, Violet Xiang, Dakota Mahan, and Nick Haber. 2025. Big-math: A large-scale, high-quality math dataset for reinforcement learning in language models. *Preprint*, arXiv:2502.17387.

Art of Problem Solving. 2024. 2024 aime i. https://artofproblemsolving.com/wiki/index.php/2024_AIME_I. Accessed: 2025-06-09.

Art of Problem Solving. 2025. 2025 aime i. https://artofproblemsolving.com/wiki/index.php/2025_AIME_I. Accessed: 2025-06-09.

Sanghwan Bae, Jiwoo Hong, Min Young Lee, Hanbyul Kim, JeongYeon Nam, and Donghyun Kwak. 2025. Online difficulty filtering for reasoning oriented reinforcement learning. *arXiv preprint arXiv:2504.03380*.

Aili Chen, Aonian Li, Bangwei Gong, Binyang Jiang, Bo Fei, Bo Yang, Boji Shan, Changqing Yu, Chao Wang, Cheng Zhu, Chengjun Xiao, Chengyu Du, Chi Zhang, Chu Qiao, Chunhao Zhang, Chunhui Du, Congchao Guo, Da Chen, Deming Ding, and 80 others. 2025a. Minimax-m1: Scaling test-time compute efficiently with lightning attention. *ArXiv*, abs/2506.13585.

Xiaoyin Chen, Jiarui Lu, Minsu Kim, Dinghuai Zhang, Jian Tang, Alexandre Piché, Nicolas Gontier, and Yoshua Bengio. 2025b. Self-evolving curriculum for llm reasoning. *arXiv preprint arXiv:2505.14970*.

Xinjie Chen, Minpeng Liao, Guoxin Chen, Chengxi Li, and Biao Fu. 2025c. From data-centric to sample-centric: Enhancing llm reasoning via progressive optimization. *arXiv preprint arXiv:2507.06573*.

Daixuan Cheng, Shaohan Huang, Xuekai Zhu, Bo Dai, Wayne Xin Zhao, Zhenliang Zhang, and Furu Wei. 2025. Reasoning with exploration: An entropy perspective. *arXiv preprint arXiv:2506.14758*.

Karl Cobbe, Vineet Kosaraju, Mohammad Bavarian, Mark Chen, Heewoo Jun, Lukasz Kaiser, Matthias Plappert, Jerry Tworek, Jacob Hilton, Reiichiro Nakano, Christopher Hesse, and John Schulman. 2021. Training verifiers to solve math word problems. *arXiv preprint arXiv:2110.14168*.

Ganqu Cui, Yuchen Zhang, Jiacheng Chen, Lifan Yuan, Zhi Wang, Yuxin Zuo, Haozhan Li, Yuchen Fan, Huayu Chen, Weize Chen, and 1 others. 2025. The entropy mechanism of reinforcement learning for reasoning language models. *arXiv preprint arXiv:2505.22617*.

Abhimanyu Dubey, Abhinav Jauhri, Abhinav Pandey, Abhishek Kadian, Ahmad Al-Dahle, Aiesha Letman, Akhil Mathur, Alan Schelten, Amy Yang, Angela Fan, and 1 others. 2024. The llama 3 herd of models. *arXiv e-prints*, pages arXiv–2407.

Daya Guo, Dejian Yang, Haowei Zhang, Junxiao Song, Ruoyu Zhang, Runxin Xu, Qihao Zhu, Shirong Ma, Peiyi Wang, Xiao Bi, and 1 others. 2025. Deepseek-r1: Incentivizing reasoning capability in llms via reinforcement learning. *arXiv preprint arXiv:2501.12948*.

Chaoqun He, Renjie Luo, Yuzhuo Bai, Shengding Hu, Zhen Leng Thai, Junhao Shen, Jinyi Hu, Xu Han, Yujie Huang, Yuxiang Zhang, and 1 others. 2024. Olympiadbench: A challenging benchmark for promoting agi with olympiad-level bilingual multimodal scientific problems. *arXiv preprint arXiv:2402.14008*.

Ehsan Kamalloo, Shipeng Li, Shikun Li, Zhiqin Yang, Xinghua Zhang, Gaode Chen, Xiaobo Xia, Hengyu Liu, and Zhe Peng. 2025. Learnalign: Reasoning data selection for reinforcement learning in llms based on improved gradient alignment. *arXiv preprint arXiv:2506.11480*.

Woosuk Kwon, Zhuohan Li, Siyuan Zhuang, Ying Sheng, Lianmin Zheng, Cody Hao Yu, Joseph E. Gonzalez, Haotong Zhang, and Ion Stoica. 2023. Efficient memory management for large language model serving with pagedattention. *Proceedings of the 29th Symposium on Operating Systems Principles*.

Kai Li, Xinggao Fan, and X. Liu. 2025. Not all rollouts are useful: Down-sampling rollouts in llm reinforcement learning. *arXiv preprint arXiv:2504.13818*.

Hunter Lightman, Vineet Kosaraju, Yura Burda, Harri Edwards, Bowen Baker, Teddy Lee, Jan Leike, John Schulman, Ilya Sutskever, and Karl Cobbe. 2023a. Let's verify step by step. *arXiv preprint arXiv:2305.20050*.

Hunter Lightman, Vineet Kosaraju, Yuri Burda, Harrison Edwards, Bowen Baker, Teddy Lee, Jan Leike, John Schulman, Ilya Sutskever, and Karl Cobbe. 2023b. Let's verify step by step. In *The Twelfth International Conference on Learning Representations*.

X Liu and 1 others. 2025. Improving data efficiency for llm reinforcement fine-tuning through difficulty-targeted online data selection and rollout replay. *arXiv preprint arXiv:2506.05316*.

Shubham Parashar, Shurui Gui, Xiner Li, Hongyi Ling, Sushil Vemuri, Blake Olson, Eric Li, Yu Zhang,

James Caverlee, Dileep Kalathil, and 1 others. 2025. Curriculum reinforcement learning from easy to hard tasks improves llm reasoning. *arXiv preprint arXiv:2506.06632*.

Yun Qu, Qi Wang, Yixiu Mao, Vincent Tao Hu, Björn Ommer, and Xiangyang Ji. 2025. Can prompt difficulty be online predicted for accelerating rl finetuning of reasoning models? *arXiv preprint arXiv:2507.04632*.

Zhihong Shao, Peiyi Wang, Qihao Zhu, Runxin Xu, Junxiao Song, Xiao Bi, Haowei Zhang, Mingchuan Zhang, YK Li, Yang Wu, and 1 others. 2024. Deepseekmath: Pushing the limits of mathematical reasoning in open language models. *arXiv preprint arXiv:2402.03300*.

Guangming Sheng, Chi Zhang, Zilingfeng Ye, Xibin Wu, Wang Zhang, Ru Zhang, Yanghua Peng, Haibin Lin, and Chuan Wu. 2025. Hybridflow: A flexible and efficient rlhf framework. In *Proceedings of the Twentieth European Conference on Computer Systems*, pages 1279–1297.

Kimi Team, Angang Du, Bofei Gao, Bowei Xing, Changjiu Jiang, Cheng Chen, Cheng Li, Chenjun Xiao, Chenzhuang Du, Chonghua Liao, and 1 others. 2025. Kimi k1. 5: Scaling reinforcement learning with llms. *arXiv preprint arXiv:2501.12599*.

Qwen Team. 2024. Qwen2 technical report. *arXiv preprint arXiv:2407.10671*.

Shenzhi Wang, Le Yu, Chang Gao, Chujie Zheng, Shixuan Liu, Rui Lu, Kai Dang, Xionghui Chen, Jianxin Yang, Zhenru Zhang, and 1 others. 2025. Beyond the 80/20 rule: High-entropy minority tokens drive effective reinforcement learning for llm reasoning. *arXiv preprint arXiv:2506.01939*.

Zhenting Wang and Cui Guofeng. 2025. Dump: Automated distribution-level data selection for rl. *arXiv preprint arXiv:2504.09710*.

Mingqi Wu, Zhihao Zhang, Qiaole Dong, Zhiheng Xi, Jun Zhao, Senjie Jin, Xiaoran Fan, Yuhao Zhou, Yanwei Fu, Qin Liu, and 1 others. 2025. Reasoning or memorization? unreliable results of reinforcement learning due to data contamination. *arXiv preprint arXiv:2507.10532*.

An Yang, Anfeng Li, Baosong Yang, Beichen Zhang, Binyuan Hui, Bo Zheng, Bowen Yu, Chang Gao, Chengen Huang, Chenxu Lv, and 1 others. 2025. Qwen3 technical report. *arXiv preprint arXiv:2505.09388*.

An Yang, Beichen Zhang, Binyuan Hui, Bofei Gao, Bowen Yu, Chengpeng Li, Dayiheng Liu, Jianhong Tu, Jingren Zhou, Junyang Lin, and 1 others. 2024. Qwen2. 5-math technical report: Toward mathematical expert model via self-improvement. *arXiv preprint arXiv:2409.12122*.

Qiying Yu, Zheng Zhang, Ruofei Zhu, Yufeng Yuan, Xiaochen Zuo, Yu Yue, Weinan Dai, Tiantian Fan, Gaohong Liu, Lingjun Liu, and 1 others. 2025. Dapo: An open-source llm reinforcement learning system at scale. *arXiv preprint arXiv:2503.14476*.

Enci Zhang, Xingang Yan, Wei Lin, Tianxiang Zhang, and Qianchun Lu. 2025. Learning like humans: Advancing llm reasoning capabilities via adaptive difficulty curriculum learning and expert-guided self-reformulation. *arXiv preprint arXiv:2505.08364*.

Haizhong Zheng, Yang Zhou, Brian R Bartoldson, Bhavya Kailkhura, Fan Lai, Jiawei Zhao, and Beidi Chen. 2025. Act only when it pays: Efficient reinforcement learning for llm reasoning via selective rollouts. *arXiv preprint arXiv:2506.02177*.

Yinmin Zhong, Zili Zhang, Bingyang Wu, Shengyu Liu, Yukun Chen, Changyi Wan, Hanpeng Hu, Lei Xia, Ranchen Ming, Yibo Zhu, and 1 others. 2024. Optimizing rlhf training for large language models with stage fusion. *arXiv preprint arXiv:2409.13221*.

Appendices

A Disclaimer on LLM Usage

The use of LLMs is permitted as a general-purpose assistance tool. In this work, LLMs were employed solely for grammar correction and sentence rephrasing. Their role was restricted to improving clarity and style; therefore, they are not considered contributors to the research.

B HIGH-PPL and LOW-PPL Prompts

As illustrated in Figure 7, HIGH-PPL prompts exhibit a greater prevalence of non-English characters relative to LOW-PPL prompts. This pattern is consistently observed across both the Qwen2.5-series and Llama model families.

Example of LOW-PPL Problems

- Cube $ABCDEFGH$, labeled as shown below, has edge length 1 and is cut by a plane passing through vertex D and the midpoints M and N of $\overline{AB}$ and $\overline{CG}$ respectively. The plane divides the cube into two solids. Find the volume of the larger of the two solids. [asy] import cse5; unitsize(8mm); pathpen=black; pair A = (0,0), B = (3.8,0), C = (5.876,1.564), D = (2.076,1.564), E = (0,3.8), F = (3.8,3.8), G = (5.876,5.364), H = (2.076,5.364), M = (1.9,0), N = (5.876,3.465); pair[] dotted = A,B,C,D,E,F,G,H,M,N; D(A–B–C–G–H–E–A); D(E–F–B); D(F–G); pathpen=dashed; D(A–D–H); D(D–C); dot(dotted); label("A",A,SW); label("B",B,S); label("C",C,SE); label("D",D,NW); label("E",E,W); label("F",F,SE); label("G",G,NE); label("H",H,NW); label("M",M,S); label("N",N,NE); [/asy]The answer is in the form
x0cracmn, where gcd(m, n) = 1. Please provide the value of m + n.

- The number $a = \frac{p}{q}$, where p and q are relatively prime positive integers, has the property that the sum of all real numbers x satisfying

$$\lfloor x \rfloor \cdot \{x\} = a \cdot x^2$$

is 420, where $\lfloor x \rfloor$ denotes the greatest integer less than or equal to x and $\{x\} =$

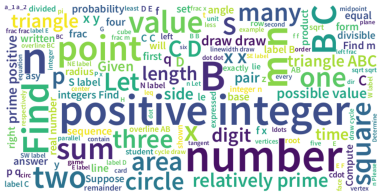

(a) LOW-PPL Prompts (Qwen2.5-7B)

(b) HIGH-PPL Prompts (Qwen2.5-7B)

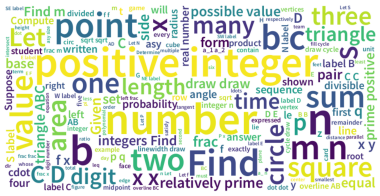

(c) LOW-PPL Prompts (Qwen2.5-Math-1.5B)

(d) HIGH-PPL Prompts (Qwen2.5-Math-1.5B)

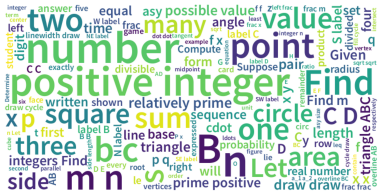

(e) LOW-PPL Prompts (Qwen2.5-Math-7B)

(f) HIGH-PPL Prompts (Qwen2.5-Math-7B)

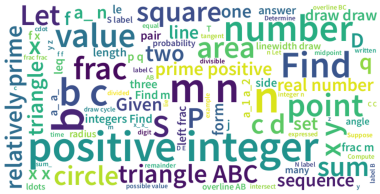

(g) LOW-PPL Prompts (Llama3.1-8B)

(h) HIGH-PPL Prompts (Llama3.1-8B)

Figure 7: Wordcloud of the Most Frequent Words in Low-/HIGH-PPL Prompts

$x - \lfloor x \rfloor$ denotes the fractional part of x. What is $p + q$?

- Let a, b be positive integers satisfying

$$\sqrt{\frac{ab}{2b^2 - a}} = \frac{a + 2b}{4b}$$

. Find $|10(a - 5)(b - 15)| + 8$.

- What is the greatest common divisor of $121^2 + 233^2 + 345^2$ and $120^2 + 232^2 + 346^2$?

Example of HIGH-PPL Problems

- At the Lexington High School, each student is given a unique five-character ID consisting of uppercase letters. Compute the number of possible IDs that contain the string "LMT".
- 设3 阶实对称矩阵A 的三个特征值分别为$-1, -1, 2$，且$(1, 1, -1)^T$ 是特征值2 所对应的特征向量. 记A 中所有元素的平方和为I，则$[I]$=_____. (English: Let the eigenvalues of A real symmetric matrix of order 3 be $-1, -1, 2$, respectively, and $(1, 1, -1)^T$be the eigenvector corresponding to eigenvalue 2. For the sum of squares of all elements in the

A I, is $[I] =$ _____.)

- 求六个元素的置换群S_6 中6 阶元素的个数。 (English: Find the number of elements of order 6 in the permutation group S_6 of six elements.)
- Three bells begin to ring simultaneously. The intervals between strikes for these bells are, respectively, $\frac{4}{3}$ seconds, $\frac{5}{3}$ seconds, and 2 seconds. Impacts that coincide in time are perceived as one. How many beats will be heard in 1 minute? (Include first and last.)

C More Training Dynamics of LOW-PPL and HIGH-PPL Prompts

For Qwen2.5-7B, Qwen2.5-Math-1.5B, and Llama3.1-8B, we found similar trends across training dynamics of LOW-PPL and HIGH-PPL groups, as shown in Figure 8, 9, and 10.

D Description of Baseline Methods

We compare PREPO against the following three baseline strategies.

- **Dynamic Sampling (DS).** Dynamic Sampling, as introduced in DAPO [Yu et al., 2025], dynamically filters out prompt groups whose generated responses all produce identical rewards (i.e., zero variance). In each training batch, DS resamples such uninformative prompt groups, thereby ensuring that the batch maintains a sufficient proportion of prompts that give meaningful gradient signals. However, it can still incur high rollout costs because many sampled prompts may remain uninformative until they are filtered.
- **Random.** The Random baseline uniformly selects prompts and associated rollouts without regard to historical feedback or variance in reward. All prompts are treated equally, so there is no mechanism to avoid rollouts on uninformative or zero-variance prompts. This method serves as a lower bound in terms of data selection sophistication.
- **GRESO.** GRESO (GRPO with Efficient Selective Rollout) [Zheng et al., 2025] is a lightweight, online, pre-rollout filtering approach. It uses statistics of reward dynamics over previous epochs to predict which prompts are likely to be uninformative (e.g., zero variance among responses) and skips them before performing rollouts.

E Code Implementation

At each global step, PPL-schedule computes perplexity on the current batch of prompts and selects the subset that matches the current progress ratio. This removes the need for tuning and avoids extra computational cost. Here is the implementation:

```
def fit(self):
    ......
    # compute perplexity for each prompt
    batch = self.actor_rollout_wg.get_ppl_batch(batch)
    # compute training progress
    rho = self.global_steps / self.total_training_steps
    # determine the prompts to select
    start_idx = math.floor((N - K) * rho)
    idx = torch.argsort(batch['ppl'])[start_idx : start_idx + K]
    # select prompts based on the indices
    batch = batch.select_via_index(idx)
    ......
```

Similarly, the relative-entropy component uses only a few lines of code, requires no manual tuning, and adds no overhead beyond the entropy computation that is already part of the existing pipeline. Here is the implementation:

```
def update_policy(self, data: DataProto):
    ......
    # all return: (bsz, response_length)
    entropy, log_prob = self._forward_micro_batch(micro_batch=data,
    temperature=temperature)
    sample_entropy = verl_F.masked_mean(entropy, response_mask, axis=1).detach()
    batch_entropy = verl_F.masked_mean(entropy, response_mask).detach()
    weight = sample_entropy/batch_entropy
    advantages *= weight[:, None]
    ......
```

F Details of Evaluation Framework

We use the `_validate()`[3] function to evaluate the model. In addition, the basic verifier is `math-verify`, and we add a LaTeX normalization package (`latex2sympy2_extended`) for the AIME and Olympiad bench.

[3]We adopt from the public Github repository: line 569 in ray_trainer.py

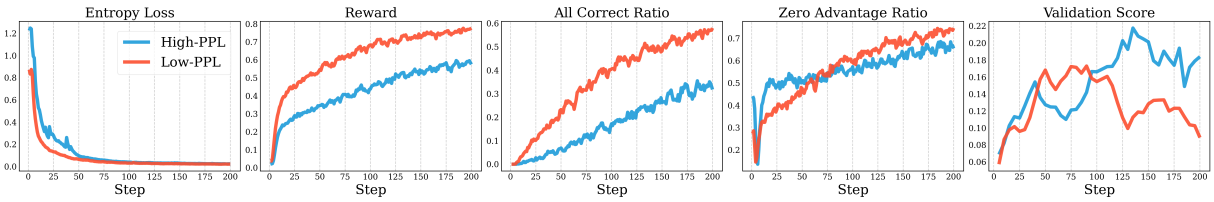

Figure 8: Training Dynamics of LOW-PPL vs. HIGH-PPL Prompts on Qwen2.5-7B.

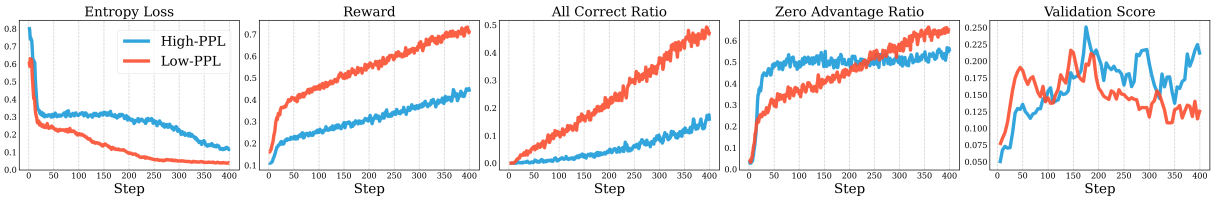

Figure 9: Training Dynamics of LOW-PPL vs. HIGH-PPL Prompts on Qwen2.5-Math-1.5B.

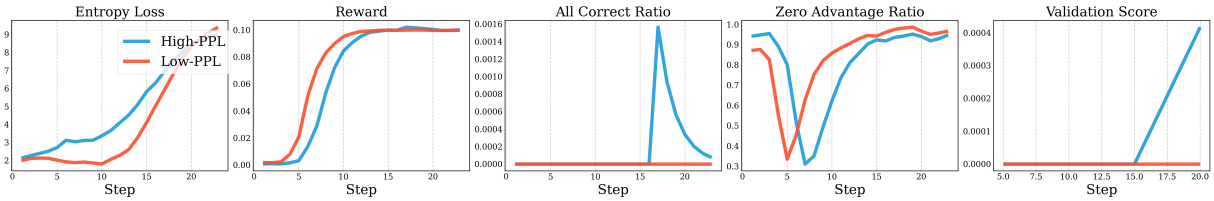

Figure 10: Training Dynamics of LOW-PPL vs. HIGH-PPL Prompts on Llama3.1-8B.

G Additional Experimental Results

In this section, we show the performance comparison between the random baseline and PREPO in Figure 11, the performance comparison across different evaluation metrics in Table 7 and the sensitivity analysis of the selection ratio in Table 8.

H Discussion

H.1 Do the Results Generalize to Other Training Datasets?

As DAPO-Math-17K contains both English and Chinese questions, prompt perplexity could correlate with language. To exclude the cofounder of language effects, we trained Qwen2.5-Math-7B on a purely English dataset selected from OpenR1-Math-220k[4], and compared PREPO with several baselines under the same training budget. The results are shown in Table 9 and the Figure 12 below. PREPO again achieves lower rollout usage while achieving a higher average performance. This indicates that the gains of PREPO are not driven by language imbalance.

H.2 What Does the PPL-schedule Contribute During Training?

We compared three configurations on Qwen2.5-Math-7B training exclusively with HIGH-PPL prompts, exclusively with LOW-PPL prompts, and the PPL-schedule, which gradually transitions from Low- to HIGH-PPL prompts. The training dynamics are shown in Figure 13.

[4] https://huggingface.co/datasets/open-r1/OpenR1-Math-220k

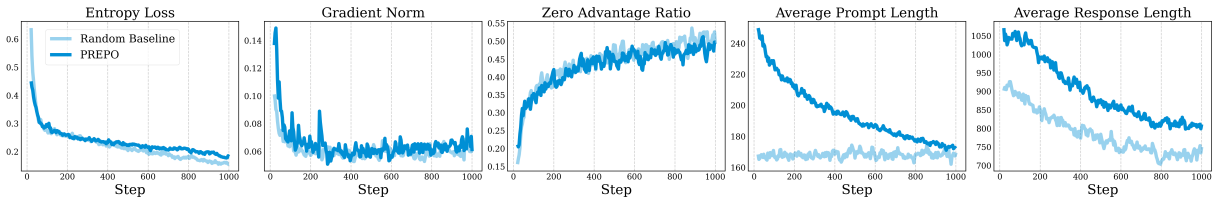

Figure 11: Full comparison between PREPO and random selection on Qwen2.5-Math-1.5B.

Table 7: Details of performance comparison (%) on Qwen models. *Avg (avg@16/32/64) means the average of AIME25 (avg@16/32/64), AIME24 (avg16/32/64), MATH, and Olympiad. Best results are highlighted in bold or underlined.*

Method	**AIME25** (avg@16)	**AIME25** (avg@32)	**AIME25** (avg@64)	**AIME24** (avg@16)	**AIME24** (avg@32)	**AIME24** (avg@64)	**Avg** ↑ (avg@16)	**Avg** ↑ (avg@32)	**Avg** ↑ (avg@64)
Qwen2.5-7B	1.25	2.60	1.17	4.17	4.90	4.95	27.69	28.21	27.87
+ DS	7.92	7.08	7.19	17.55	15.00	14.90	34.97	34.76	34.13
+ Random	6.98	6.35	6.51	16.41	15.63	15.89	34.39	34.04	34.14
+ GRESO	9.22	7.29	7.50	10.83	13.65	13.39	34.39	34.92	34.90
+ PREPO (Ours)	10.21	10.62	10.00	16.09	15.52	16.35	**35.61**	**35.72**	**35.63**
Qwen2.5-Math-1.5B	3.54	3.75	4.48	10.21	8.33	8.96	24.23	23.81	24.15
+ DS	10.83	13.76	14.54	25.83	21.72	23.04	34.10	33.80	34.33
+ Random	20.00	17.45	18.81	16.67	15.42	16.50	35.86	34.91	35.52
+ GRESO	15.38	11.40	15.39	20.00	19.20	17.97	34.16	32.86	33.56
+ PREPO (Ours)	20.00	19.69	19.38	16.67	16.98	17.03	**36.23**	**36.23**	**36.17**
Qwen2.5-Math-7B	8.95	9.17	8.80	17.50	20.80	19.22	35.45	35.45	34.96
+ DS	13.33	14.27	14.84	33.33	35.63	34.69	34.10	40.36	40.26
+ Random	10.00	12.50	12.50	26.67	29.34	29.87	35.86	40.73	40.86
+ GRESO	18.33	18.58	18.58	25.83	24.38	25.00	37.46	36.90	37.05
+ PREPO (Ours)	12.81	14.41	15.93	26.15	29.17	29.25	**39.59**	**40.75**	**41.15**
Qwen3-4B	30.00	47.30	44.89	53.33	61.60	28.70	57.53	63.92	55.09
+ DS	63.33	53.90	54.80	66.67	63.50	65.30	70.78	67.63	68.30
+ Random	60.00	58.85	60.16	70.00	65.73	64.69	71.33	69.98	70.05
+ GRESO	56.67	58.33	57.24	69.17	71.77	69.79	69.89	70.96	70.19
+ PREPO (Ours)	66.67	62.19	63.39	80.00	74.28	77.45	**75.99**	**73.44**	**74.53**

Table 8: Performance Comparison (%) of PREPO with Different Selction Ratio ($K/\mathcal{B}$, $\mathcal{B}$ fixed) on Qwen2.5-Math-1.5B. *Best results are highlighted in bold or underlined.*

Selection Ratio	**AIME25**	**AIME24**	**MATH**	**Olympiad**	**Avg** ↑	**# Rollouts** ↓
30%	20.00	20.83	75.85	25.00	35.42	1.4M
25%	13.33	20.00	73.55	24.00	32.72	1.5M
20%	20.00	16.67	76.25	32.00	**36.23**	**1.1M**
15%	13.33	20.00	75.75	22.17	32.81	1.4M
10%	15.83	19.17	70.25	21.33	31.65	1.7M
5%	19.17	16.67	69.85	20.17	31.46	1.8M

Table 9: Comparison of PREPO and baselines trained on all-English data (Model: Qwen2.5-Math-7B)

Method	**AIME25**	**AIME24**	**MATH**	**Olympiad**	**Avg** ↑	**#Rollout** ↓
DS	11.98	30.00	72.80	42.02	39.20	3256K
Random	10.79	28.25	80.21	36.72	38.99	2457K
GRESO	6.67	30.00	79.20	45.63	40.38	1331K
PREPO	12.92	33.33	78.05	44.10	**42.10**	**860K**

In terms of entropy loss, the PPL-schedule achieves a balance between the two extremes: entropy decreases steadily but not excessively, thereby mitigating the risk of collapse. With re-

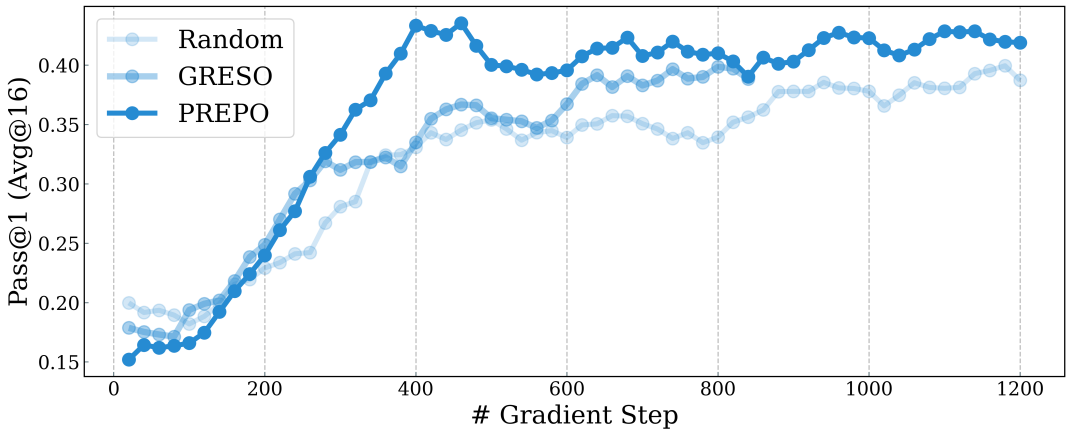

Figure 12: Comparison of performances across PREPO, GRESO, and Random (x-axis: training step, y-axis: validation score, model: Qwen2.5-Math-7B, training data: OpenR1-Math)

spect to the zero-advantage ratio, the PPL-schedule consistently maintains a lower value, ensuring that a greater proportion of rollouts remain informative throughout training.

H.3 What Does Relative Entropy Bring to Training?

As shown in Figure 14, PREPO with relative entropy further reduces the zero-advantage ratio, thereby improving sample efficiency.

Case Analysis. In Figure 15, we display examples of responses with their token-level entropy from the same mini-batch, where darker colors mean higher entropy, and each sequence is weighted by its relative entropy.

H.4 Does Prompt Perplexity Change During Training?

As shown in Figure 16, we computed the PPL range at each training epoch and observed that it remained relatively stable throughout training. In addition, the PPL of the prompts used for training exhibited minimal variation.

H.5 What Is the Time Cost of PREPO?

As shown in Figure 17, the time consumption of calculating prompt PPL is barely minimal compared to the rollout generation duration.

H.6 How Does PREPO Affect Problem Diversity?

The analysis indicates that PREPO selects a more diverse set of problems than random sampling. Specifically, PREPO achieves broader coverage across Mathematics Subject Classification[5] (MSC) categories during training, as illustrated in Figure 18.

H.7 How Does PREPO Compare to Training Without Filtering?

For Qwen2.5-Math-7B, we observe that PREPO attains performance comparable to training on the full dataset without any filtering, i.e., using 5 times rollouts per step, as shown in Figure 19. The "Less is More" pattern implies that efficient selection can reduce the amount of data needed for RLVR training.

H.8 Does PREPO Lead to Memorization of Training Data?

Following Wu et al. [2025], we trimmed 40% of each prompt to construct *partial problems*. We then evaluate models on these partial prompts and compute the average pass rate of 16 generations. As shown in Figure 20, the vast majority of partial problems have near-zero pass rate, with only a small fraction achieving non-trivial success. These distributions suggest that the model does not merely memorize the training data but instead requires the full problem context to solve tasks.

H.9 How Sensitive Is PREPO to Extreme Entropy Values?

Since $w_i = \bar{H}_i/\bar{H}$ is normalized by the batch mean, a rollout with $\bar{H}_j \gg \bar{H}$ has a large weight $w_j \gg 1$, while simultaneously reducing the weights of the others ($w_i \ll 1$ for $i \neq j$). The

[5] MSC : https://zbmath.org/classification/

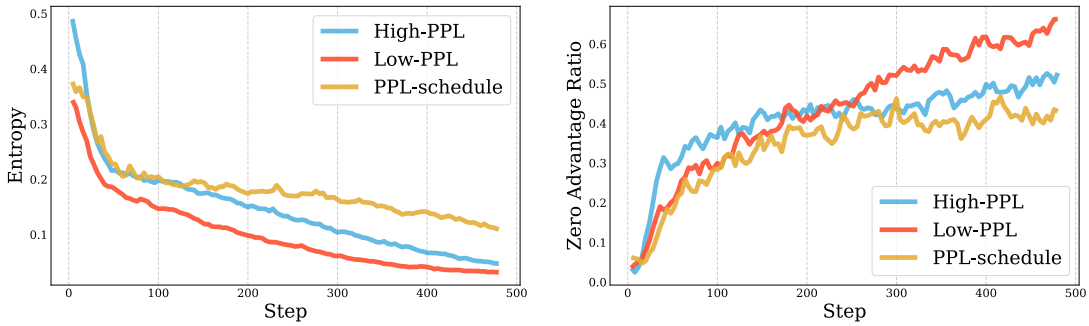

(a) Entropy (b) Zero Advantage Ratio

Figure 13: Comparison of Training Dynamics between PPL-schedule and Static PPL Selection (Low- and HIGH-PPL groups)

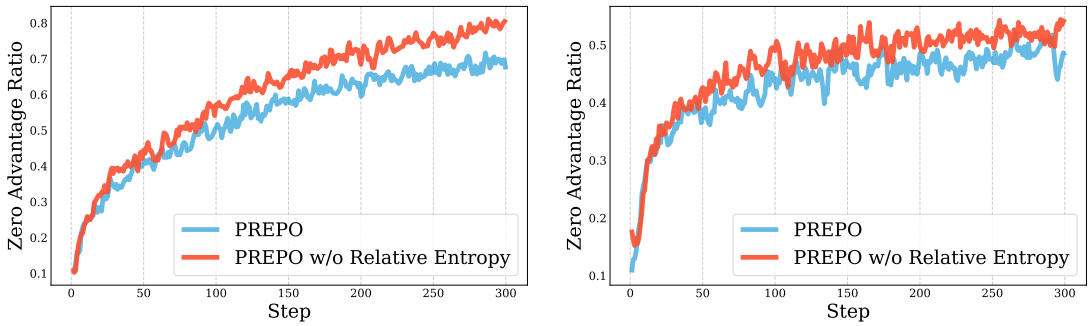

(a) Qwen2.5-Math-7B (b) Qwen2.5-Math-1.5B

Figure 14: Comparison of zero advantage ratio between PPL-schedule and PREPO.

derivative

$$\frac{\partial w_i}{\partial \bar{H}_j} = \begin{cases} \dfrac{1}{\bar{H}} - \dfrac{\bar{H}_j}{\bar{H}^2} \dfrac{|o_j|}{\sum_k |o_k|}, & i = j, \\ -\dfrac{\bar{H}_i}{\bar{H}^2} \dfrac{|o_j|}{\sum_k |o_k|}, & i \neq j, \end{cases}$$

clarifies this behavior: (1) for $i = j$, the two terms partially cancel, so although w_j is already large, its growth rate is moderated as $\bar{H}_j$ increases further; (2) for $i \neq j$, the derivative is negative, confirming that a large $\bar{H}_j$ suppresses the weights of all other rollouts. Empirically, such outliers are rare. As shown in Figure 21, the distribution of relative entropy weights remains stable mainly across training steps 100, 200, 300, and 400 for Qwen2.5-Math-1.5B, where most rollouts clustered near one, with negligible mass on extreme values.

(a) Correct answer
x1.65

(b) Incorrect answer
x1.33

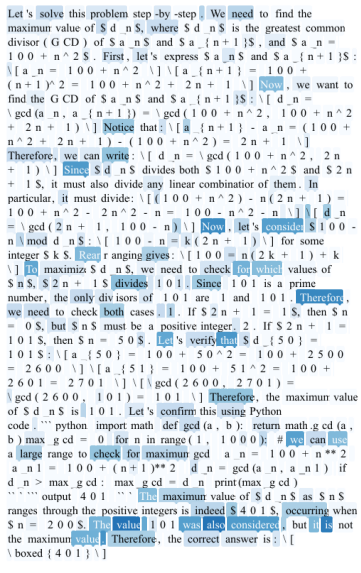

(c) Correct answer
x0.73

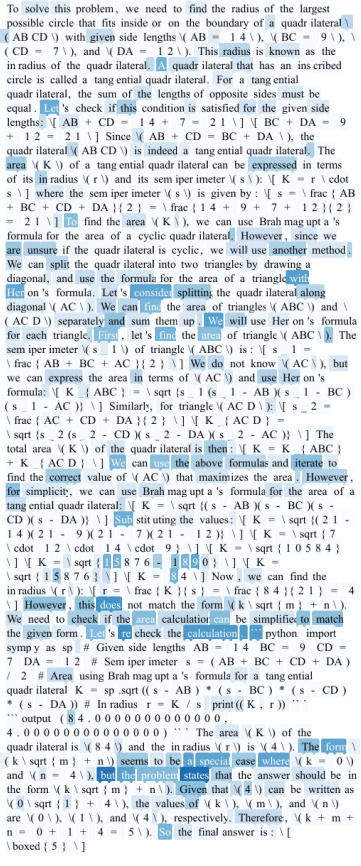

(d) Incorrect answer
x0.74

Figure 15: Token-Level Entropy of Sequences within A Mini-batch (with Relative-Entropy in Red).

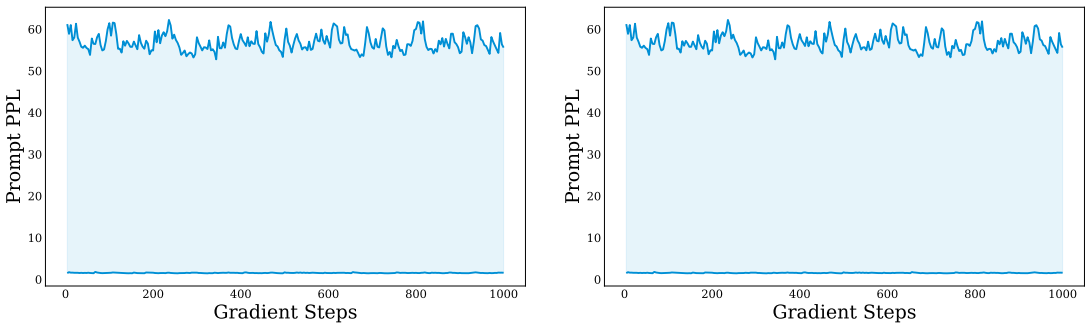

(a) Qwen2.5-Math-7B (b) Qwen2.5-Math-1.5B

Figure 16: Range of prompt PPL during training.

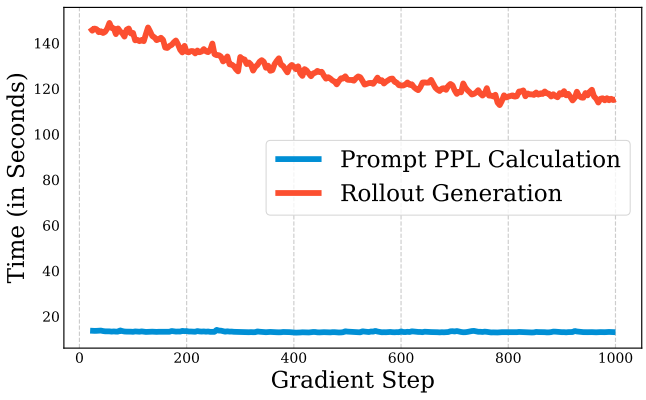

Figure 17: Comparison of calculating prompt PPL and rollout generation

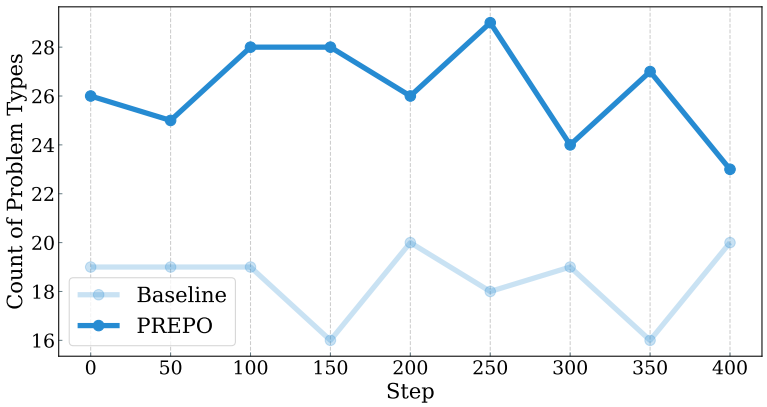

(a) Unique number of MSC tags

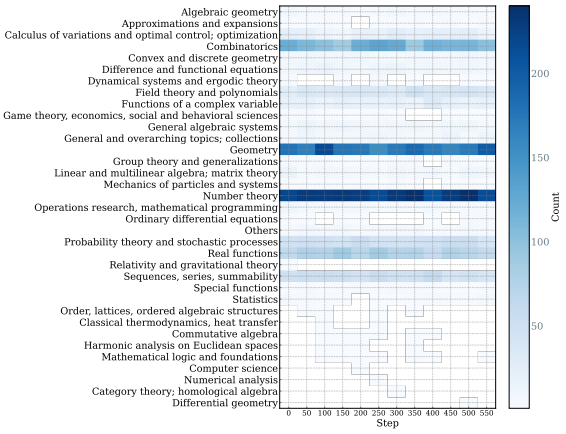

(b) MSC frequency of PREPO

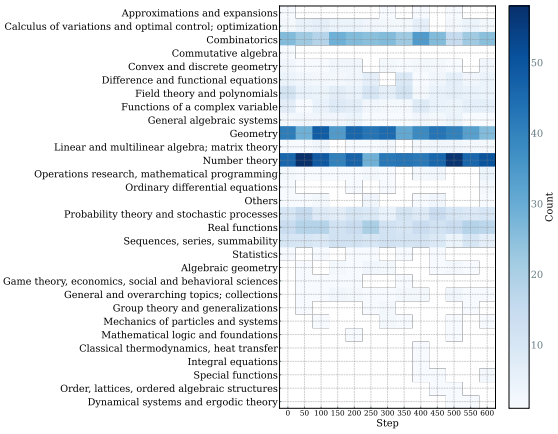

(c) MSC frequency of baseline (random)

Figure 18: Comparison of problem diversity between PREPO and baseline on Qwen2.5-Math-7B.

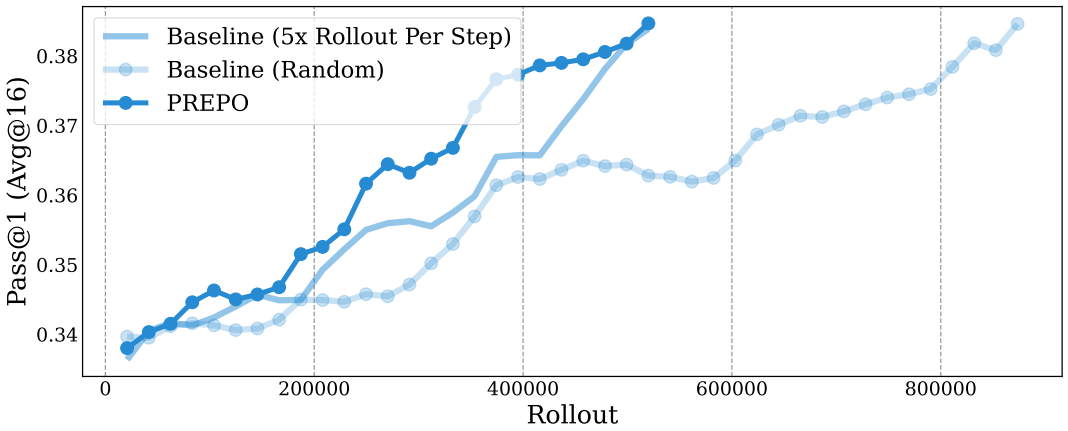

Figure 19: Comparison of PREPO and baselines (a) training w/o filtering (b) random selection.

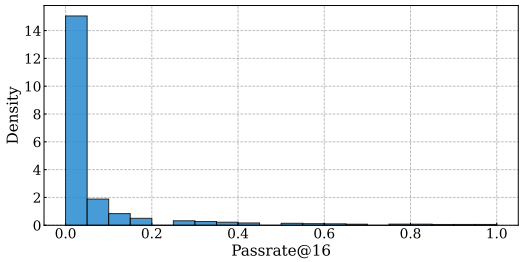

(a) Qwen2.5-Math-1.5B

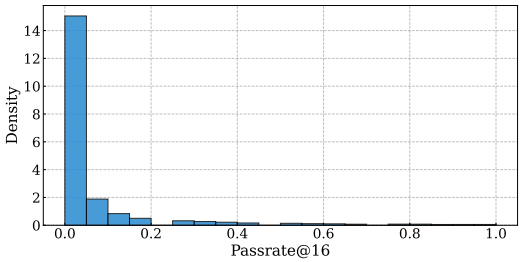

(b) Qwen2.5-Math-7B

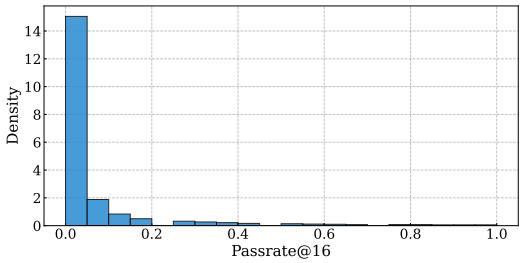

(c) Qwen3-4B

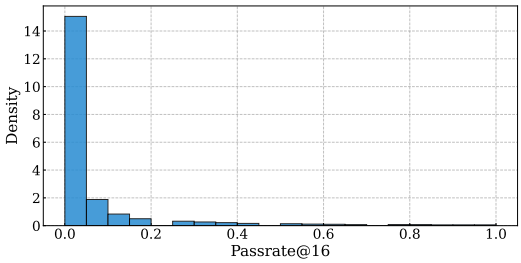

(d) Llama3.1-8B

Figure 20: Distribution of passrate@16 over all partial prompts

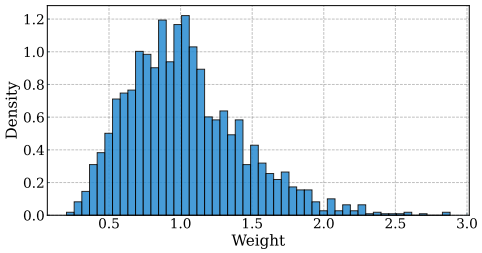

(a) Step 100

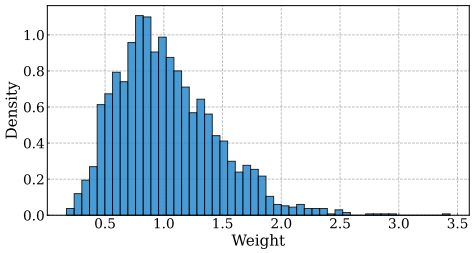

(b) Step 200

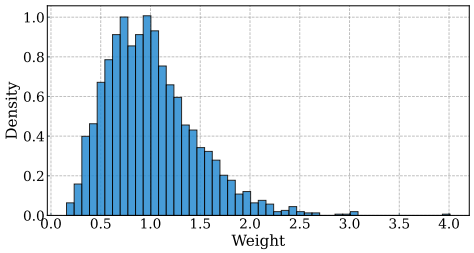

(c) Step 300

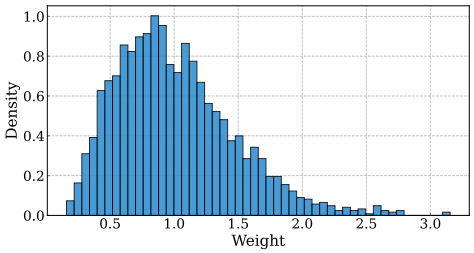

(d) Step 400

Figure 21: Weight Distribution During Training (Qwen2.5-Math-1.5B).